Japanese Journal of Applied Physics

The Japan Society of Applied Physics

ACCEPTED MANUSCRIPT

Simple method of measuring thicknesses of surface-hardened layers by laser ultrasonic technique

To cite this article before publication: Yong Lee *et al* 2021 *Jpn. J. Appl. Phys.* in press https://doi.org/10.35848/1347-4065/ac030f

Simple method of measuring thicknesses of surface-hardened layers by laser ultrasonic technique

Yong Lee[1]*, So Kitazawa[2], and Rikesh Patel[3]

[1]*Research & Development Group, Hitachi, Ltd., Kokubunji-shi, Tokyo 185-8601, Japan*

[2] *Research & Development Group, Hitachi, Ltd., Hitachi-shi, Ibaraki 319-1292, Japan*

[3]*Optics and Photonics Research Group, Faculty of Engineering, University of Nottingham, Nottingham NG7 2RD, UK*

E-mail: yong.lee.ak@hitachi.com

We proposed a simple non-contact inspection method using a laser ultrasonic technique to measure the thickness of a surface-hardened layer. This measurement is based on the dependence of a surface-wave velocity on the thickness of the hardened layers. In this case, it is essential to measure the surface-wave velocity with a wavelength comparable to the thickness of a hardened layer. However, it is not easy to selectively generate the surface waves with a desired wavelength. Thus we proposed the method where the surface waves with a desired wavelength are extracted using electrical bandpass filters. This method is simpler than the conventional one based on dispersion because the surface-wave velocity is directly obtained from measured temporal waveforms. We applied the method to measure the thickness of hardened layers and showed that the results were in good agreement with that obtained by the conventional method and numerical results.

1. Introduction

Steel products such as automobile parts are typically surface-hardened to improve their abrasion resistance and fatigue properties. There are induction hardening, carburizing and quenching hardening, and nitriding treatments as surface-hardening techniques. Since the thicknesses of surface-hardened layers have an impact on the characteristics of abrasion resistance and fatigue, they must have a surface-hardened layer of optimum thickness. Therefore, the thickness of the surface-hardened layer must be measured as accurately as possible.

Random inspection of the thickness of a surface-hardened layer is currently dominant and utilizes a destructive technique. The destructive way requires considerable effort and is time-consuming. Therefore, a nondestructive, non-contact thickness measurement technique is preferable because it can potentially achieve a full inspection compared to currently dominant random inspections. Several nondestructive, surface-hardened-layer thickness (hardened-layer thickness, below) gauges based on conventional ultrasonic transducers, the Eddy current method, and a potentiometer have been developed.[1-4)] Only the Eddy current method is contactless among them; however, the gap between the probe and the specimen is small in the order of millimeters, and the measurement accuracy is sensitive to the gap.

The laser ultrasonic technique (laser UT) has been receiving much attention as a non-contact, nondestructive detection technique for many applications, such as flaw detection and characterization of a medium.[5-19)] Laser UT utilizes irradiation of a high-power short-pulse laser to induce ultrasonic waves by a thermoelastic mode (damage-free) or an ablation mode and ultrasonic displacement measurement with a laser. Besides a non-contact detection, there are many attractive qualities in laser UT, such as 1) increased detection speed, 2) in situ measurements in an industrial setting, 3) a small footprint, 4) a broadband system (kHz−GHz), and 5) curved-complex-surface detection. However, at the present stage, laser UT systems are large and expensive because they utilize a large, expensive conventional adaptive receiver based on two-wave mixing[20,21)] Recently, a compact, low-cost receiver based on a knife-edge method called speckle knife-edge detector (SKED) was developed[22,23)], and it has become a key component in providing a compact, low-cost laser UT system.

Laser ultrasonic technique is useful for measuring surface properties because of the efficient generation and reception of surface waves. Information obtained from surface-wave

measurement can be deduced about the thickness of case hardening and protective coatings.[24-30] In this paper, we applied the laser UT system using the SKED laser UT to measure hardened- layer thickness. The principle of the measurement technique utilizes a surface-wave velocity's dependence on hardened-layer thickness. We found that there is a strong correlation between the surface-wave velocity and the hardened-layer thickness if the wavelength of the surface wave is comparable to the hardened-layer thickness because the penetration depth of the surface wave is nearly equal to its wavelength. Thus, we must evaluate the velocity of the surface wave with an optimum wavelength for an accurate measurement of the hardened-layer thickness. However, a laser-induced ultrasonic wave has a broadband spectrum and can extract the velocity of the necessary surface wave from the measured results. A conventional method based on numerical analysis includes a spectral decomposition process that obtains a phase velocity dispersion and parameter fitting process. [27,28] This is time-consuming and unsuitable for a full inspection. We propose an alternative method that is based on spectral extraction using an electrical bandpass filter. This is simpler than the conventional method because the velocity of the desired surface wave is directly obtained from measured temporal waveforms. We demonstrate the feasibility of our technique by applying it to measuring the thickness of carburizing and quenching hardened layers.

2. Simple numerical results

We calculated the surface-wave velocity's dependence on the hardened-layer thickness in a simple way. The skin depth of a surface wave (mostly Rayleigh wave) is known to nearly equal its wavelength (see Fig. 1). The energy distribution function of the surface wave in the depth (z) direction: R(f, z) is approximated by

$$R(f,z) = \frac{2}{\lambda(f)} exp\left(\frac{-2z}{\lambda(f)}\right), \quad (1)$$

where f is a frequency and λ is a wavelength. A surface-wave velocity in a specimen with a hardened layer: v(d, f) is given by

$$v(d,f) = \big(1 - p(d,f)\big)v_0 + p(d,f)v_1, \quad (2)$$

where p(d, f) is the ratio of the energy of the surface wave in the hardened layer to its total energy described by Eq. (3), d is the thickness of the hardened layer, v_0 is a surface-wave velocity in a base material, and v_1 is a surface-wave velocity in the hardened layer.

$$p(d,f) = \int_0^d R(f,z)\, dz \quad (3)$$

A temporal ultrasonic wave generated by a short-pulse laser is pulse-shaped, and its frequency spectrum is widely broadened. Therefore, the surface-wave velocity: v(d,f) needs to be averaged over the frequency in the following way.

$$\bar{v}(d) = \int_0^\infty \mathrm{v(d,f)S(f)\ df} \quad (4)$$

S(f) is the frequency spectrum of the surface wave given by

$$S(f) = \frac{1}{\sqrt{2\pi}\sigma} exp\left[\frac{-(f-f_c)^2}{2\sigma^2}\right], \quad (5)$$

where f_c is a central frequency, FWHM is a full width at a half maximum and σ is expressed by

$$\sigma = \frac{FWHM}{2\sqrt{2ln2}}\ . \quad (6)$$

Figure 2 shows numerical examples calculated using the above equations for various frequency spectra of surface ultrasonic waves (surface waves below): (1) f_c=1 MHz, FWHM=0.4 MHz, (2) f_c=2 MHz, FWHM=1 MHz, and (3) f_c=4 MHz, FWHM=3.5 MHz. The maximum layer thickness of 3 mm is a typical thickness of a hardened layer fabricated by a carburizing and quenching hardening process. The numerical results shown in Fig. 2 indicate that the surface-wave velocity is highly dependent on the hardened-layer thickness in the wide range of thicknesses for the small f_c and FWHM.

In this calculation, we assumed that the interface between the hardened layer and the base material (steel) is steeply changed although it is actually gradually changed. We believed that the assumption is enough for the purpose of this paper. However, taking account of the gradual interface will be necessary to improve the calculation accuracy. It remains for future work.

The f_c and FWHM of laser-induced surface waves depend on a pulse length, a beam spot size and material thermal properties. It is known that the temporal waveform of the surface wave becomes broader with increasing the beam spot size. This broadening comes from a delay in the arrival of the signal caused by the energy deposition spreading in space dimension.[31] This means that the f_c and FWHM can be controlled by changing the beam spot size. We reported about the measurement of the hardened-layer thickness using the control of the f_c and FWHM by the beam spot size.[32] Therefore, it is beyond the scope of this article.

3. Experimental setup

An experimental setup is illustrated in Fig. 3 (a). The surface wave was generated by a Q-switched YAG laser, emitting pulses of a length of 10 nsec and a pulse energy of 10 mJ. A line excitation scheme was used by focusing the laser beam onto the surface of the specimens with a cylindrical lens after expanding the beam. The detector used in this experiment is a SKED based on a knife-edge detector (KED) (or optical beam deflection) that detects a passing ultrasonic wave using a laser.[3)] A major problem with the KED is detecting the ultrasonic waves from a rough surface. When an optically rough surface is irradiated with laser beams, light scattering creates interference in the form of a so-called speckle pattern. This speckle pattern significantly reduces the sensitivity of the KED. The SKED is innovative technology that overcomes this, and it is a modified conventional KED implemented on a CMOS integrated circuit that enables us to reorganize the light reflected from a rough surface to behave as if the reflection were from a smooth surface. A detection laser for the SKED is a CW laser with a wavelength of 532 nm that is half that of the generation laser.

This laser ultrasonic testing system called SKED laser UT was used for all the experiments described in this paper. Surface waves generated by the laser were measured at various spacings between two laser beams: L (shown in Fig. 3 (b)), starting from 9 mm to 25 mm away from the line source with a step size of 4 mm.

4. Experimental results obtained by a dispersion technique

The samples used in our experiments were carburized and quenched steel with different thicknesses ranging from 0 to 3 mm. Their size is 15 mm x 30 mm. Two samples with the same thickness (made by the same process) were fabricated, and one of the two was used to measure the thickness of the hardened layer by measuring the hardness with destructive inspection. Figure 4 shows temporal ultrasonic waveforms measured by the SKED laser UT system. The largest peak signal is the surface wave propagated directly from the line source. The second and third largest peaks are reflected waves from the left and right sample edges, respectively. The attenuation rates of the amplitudes of the surface waves were less than fifty percent. Thus, the observed signals were large enough to get a large signal-to-noise ratio.

The energy of a surface wave is concentrated within a penetration depth of the order of its wavelength. This means that the surface-wave velocity is governed by the elastic property of the material depth it probes. For a multilayer medium of different elastic properties, the propagating wave is influenced by all the layers it probes, resulting in a dispersed wave. A frequency dependent phase velocity of the dispersed wave—namely, the dispersion curve in general—is used to determine the layer thickness.[27,28)]

To obtain the experimental dispersion curve, the generated surface waves were measured for two different spacings, L_1 and L_2. They were Fourier-transformed, then the phase difference between the two waves, $\Delta\varphi_{12}(f)$, was determined from the unwrapped phase angle of the Fourier spectrum.[5)] The dispersion curve: $v_{12}(f)$ was obtained by inserting $\Delta\varphi_{12}(f)$ into Eq. (7).

$$v_{12}(f) = 2\pi f \frac{L_2 - L_1}{\Delta\varphi_{12}(f)} \tag{7}$$

In this experiment, five waveforms for different spacings L_i (i=1~5) were measured (as shown in Fig. 4) and averaged four dispersion curves: $v_{i,i+1}$ (f) (i=1~4) to obtain $\bar{v}(f)$.

$$\bar{v}(f) = \frac{1}{4}\sum_{i=1}^{4} v_{i,i+1}(f) \tag{8}$$

Figures 5 (a), (b), and (c) show the broadband spectrum of the surface wave in the SKED laser UT system and examples of the power spectrum calculated from the temporal waveform, its frequency-dependent phase angle, and its unwrapped frequency-dependent phase angle. Figure 6 shows an example of averaged phase velocity dispersion curves for several samples whose thicknesses of hardened layers are 0, 2.1 mm, 2.6 mm, and 3 mm. It shows the dispersive frequency region up to 3 MHz. The sample without the hardened layer is not dispersive. On the other hand, the others show dispersive behavior in a low-frequency region. Furthermore, The phase velocity decreases as the hardened layer thickness increases. This trend reveals the surface-wave velocity in the sample with the hardened layer depends on the hardened layer thickness.

Figure 7 shows the experimental and calculated results of surface-wave velocity as a function of hardened layer thickness. Three experimental results were obtained by averaging the phase velocity over different frequency regions. They were averaged over the spectra used in the calculation. In this calculation, the surface-wave velocities of the base material

and the hardened layer, v_0 and v_1, are assumed to be 3.017 mm/μsec and 2.94 mm/μsec, respectively. The value of v_0 was determined by the velocity of the sample without the hardened layer. The value of v_1 was used as a fitting parameter. The values of v_0 and v_1 are similar to those in Ref. [2]. The f_c and FWHM used in the calculation were determined from the experimental results obtained in the proposed scheme described later (shown in Fig. 9) . The surface-wave velocity is more strongly correlated with the hardened layer thicknesses, as it is averaged over the lower frequency region. This behavior agrees well with the calculated results.

This dispersion technique is slightly different from the technique described in Refs. [27] and [28]. In Refs. [27] and [28], the velocity dispersion curve fitting between theoretical calculation and experimental results is performed to evaluate a coating layer thickness. In this dispersion technique, the surface-wave velocity in a certain frequency region is extracted from the velocity dispersion curve to obtain the hardened layer thickness by using a curve of the surface-wave velocity versus hardened layer thickness obtained in advance.

5. Experimental results obtained by the proposed technique

An alternative way to select a moderate frequency region of the surface wave to determine the hardened layer thickness is to use electrical frequency filters. We used low-pass filters to only extract signals with lower frequency components. The low-pass filters were placed before placing an electrical amplifier and an oscilloscope. Their cutoff frequencies were 1 MHz and 1.7 MHz. Figures 8 (a) , (b), and (c) show temporal waveforms of surface waves as a function of a spacing between two beams obtained with a 1-MHz cutoff frequency filter, a 1.7-MHz cutoff frequency filter, and no filter, respectively. The corresponding frequency spectra are shown in Fig. 9. The frequency-filtered waveforms (Figs. 8 (a) and (b)) still show their peak shapes; therefore, it is possible to simply obtain the surface-wave velocities by the propagation speed of the peak shapes. The velocities were obtained from the largest peak propagations. Appropriate bandwidth is necessary for the waveform to have a peak shape. Otherwise, the waveform becomes like a sinusoidal wave, and it is relatively difficult to obtain the surface-wave velocity from the waveform's time-of-flight.

The obtained surface-wave velocities were plotted as a function of hardened layer thickness and compared with the calculated results, shown in Fig 10. The experimental results show good agreement with the calculated ones, as is the case in the conventional technique. In our proposed technique, the surface-wave velocity is simply obtained from a waveform's time-of-flight, unlike the conventional technique in which a relatively complicated calculation is necessary to obtain the surface-wave velocity.

Velocity measurement errors mainly come from timing jitters of the generation laser. The timing jitters of the generation laser used in this experiment is 1.5 nsec, leading to the error of about ± 0.001 mm/μsec.

6. Conclusions

We applied our scheme based on a laser ultrasonic technique of measuring the thickness of a surface-hardened layer. Electrical frequency filters implemented in this scheme select the low-frequency components of laser-induced surface ultrasonic waves to measure a millimeter-order hardened layer with high accuracy. Compared with the conventional method, this method saves time because the velocity of a low-frequency surface wave is obtained directly from temporal waveform data. Improving the measurement accuracy and reproducibility are left for future work.

References

1) H. Tanaka and Y. Oukubo, Tetsu to hagane, **77,** p.100 (1991) [in Japanese].
2) A. Terakubo and T. Arakawa, IIC Review **55**, p. 52 (2016) [in Japanese].
3) J. M. Szlagowska-Spychalska et al. NDT&E International **54**, p. 56 (2013).
4) N. Iwata and N. Kato, Kensa Gijutsu, **15**, p.76 (2010) [in Japanese].
5) C. B. Scruby and L. E. Drain, Laser Ultrasonics Techniques and Applications, Adam Hilger, Bristol, England, 1990.
6) S. Yamamoto et al., Materials Transactions **55**, p. 998 (2014).
7) A. Cavuto, et al., Ultrasonics **55**, p. 48 (2015).
8) Y. Kurozumi et al., INSS JOURNAL **19**, p. 183 (2012) [in Japanese].

9) Y. Shimada et al., Laser Review **38**, p. 749 (2010) [in Japanese].
10) Y. An, et al., Smart Material and Structures **23**, p. 1 (2014).
11) M. Sano, et al., Procedia Engineering, **81**, p. 1414 (2014).
12) J. Takatsubo et al., Journal of the Japanese Society for Non-Destructive Inspection **63**, p.142 (2014) [in Japanese].
13) Y. K. An et al, Smart Mater. **23** 095019 (2014).
14) M. Arone et al., J. Mater. Process. Technol. **176**, p. 95 (2006).
15) A. Cavuto et al., Ultrasonics **55**, p. 48 (2015).
16) D. Cerniglia et al., Ultrasonics **62**, p. 292 (2015)
17) B. Dutton et al., NDT&E International **44**, p. 353 (2011).
18) M. S. Harb and F. G. Yuan, Ultrasonics **64** p. 162 (2016).
19) T. Hayashi et al., J. Acoust. Soc. Am. 126, p. 1101 (2009).
20) R. K. Ing and J. P. Monchalin, Appl. Phys. Lett. 59, p. 3233 (1991)
21) R. J. Dewhurst et al., Meas. Sci. Technol. **10**, p. 139 (1999).
22) M. Clark, Journal of Physics: Conferences Series **278**, 012025, (2011).
23) S. D. Sharples et al., Journal of Physics: Conferences Series **520**, 012004, (2014).
24) C. B. Scruby, Ultrasonics **27**, p. 197 (1989).
25) T. W. Murray et al., Appl. Phys. Lett. **74**, p. 3561 (1991).
26) A. Neubrand and P. Hess, J. Appl. Phys. 71, p. 227 (1992)
27) H. I. Ringermacher et al., Review of Progress in Quantitative Nondestructive Evaluation **12**, p. 549 (1993).
28) X. R. Zhang et al., Analytical Sciences **17**, p. 223 (2001).
29) H. C. Wang et al., Optics Express **17**, p. 15593 (2009).
30) C. H. Yeh et al., Physics Procedia **70**, p. 492 (2015).
31) B. Xu et al., J. Appl. Phys. **99**, 033508 (2006).
32) Y. Lee et al., The 68th JSAP spring meeting, 17a-Z13-5 (2021).

Figure Captions

Fig. 1. Schematic of propagating surface ultrasonic wave in a surface-hardened sample and the surface-wave energy distribution in the depth direction. λ denotes a wavelength of the surface wave.

Fig. 2. Calculated surface-wave velocities as a function of a hardened layer thickness for various spectra.

Fig. 3. Schematics of (a) experimental setup of SKED laser UT (overhead view) and (b) excitation scheme.

Fig. 4. Example of temporal waveforms of surface waves as a function of the propagation distance. L denotes the propagation distance.

Fig. 5. (a) Typical spectrum of a surface ultrasonic wave, frequency-dependent phases (b) before unwrap and (c) after unwrap.

Fig. 6. Example of averaged phase velocity dispersion curves for several samples. d denotes a thickness of the hardened layer.

Fig. 7. Surface-wave velocity as a function of hardened layer thickness obtained by a phase velocity dispersion technique. Circles are experimental results; lines are calculated results.

Fig. 8. Temporal waveforms of surface waves as a function of the propagation distance obtained with (a) 1-MHz cutoff frequency filter, (b) 1.7-MHz cutoff frequency filter, and (c) no filter. L denotes the propagation distance.

Fig. 9. Spectra of the surface waves obtained with (a) no filter, (b) 1.7-MHz cutoff frequency filter, and (c) 1-MHz cutoff frequency filter.

Fig. 10. Surface-wave velocity as a function of hardened layer thickness obtained by the proposed technique. Circles are experimental results; lines are calculated results. LPF denotes a low-pass filter.

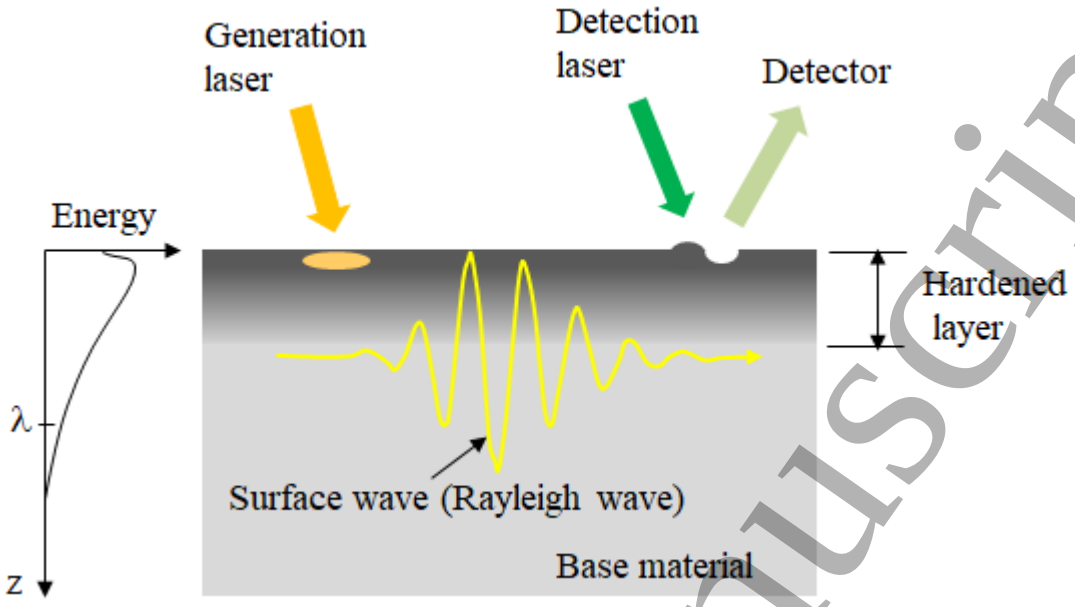

Fig. 1.

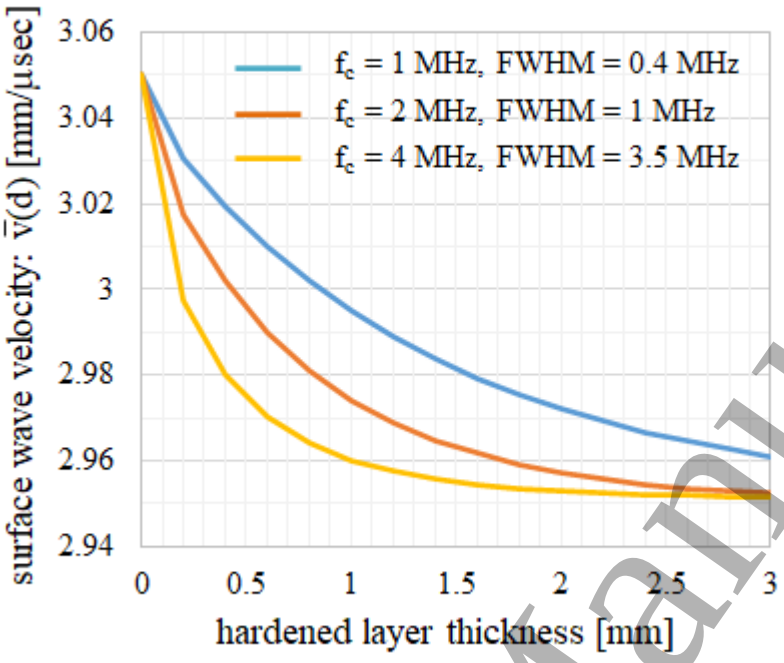

Fig. 2.

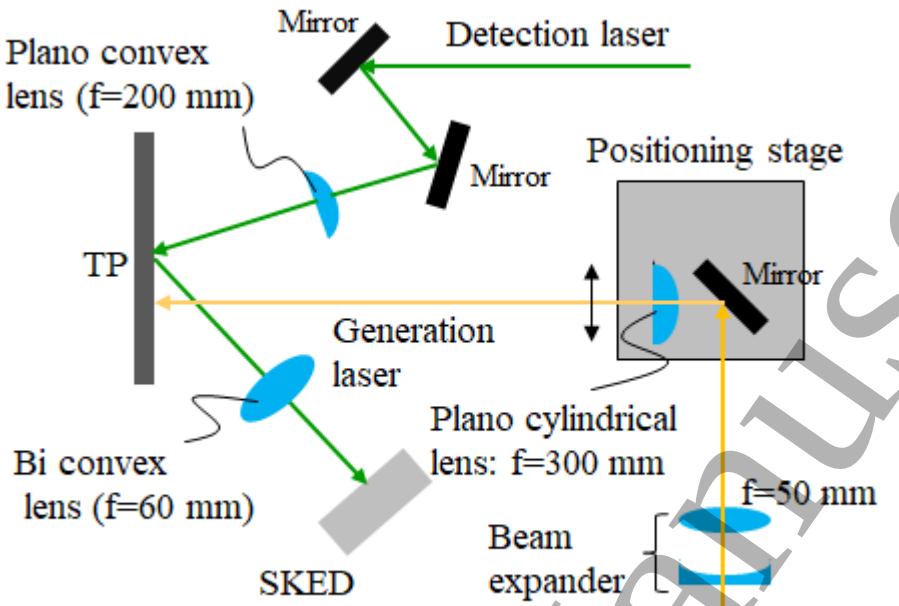

(a)

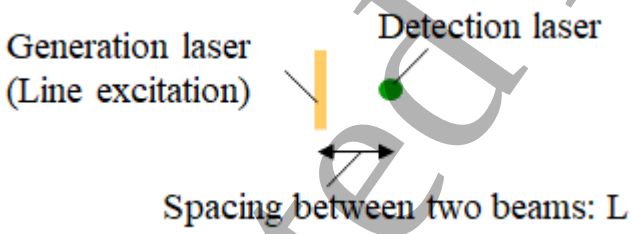

(b)

Fig. 3.

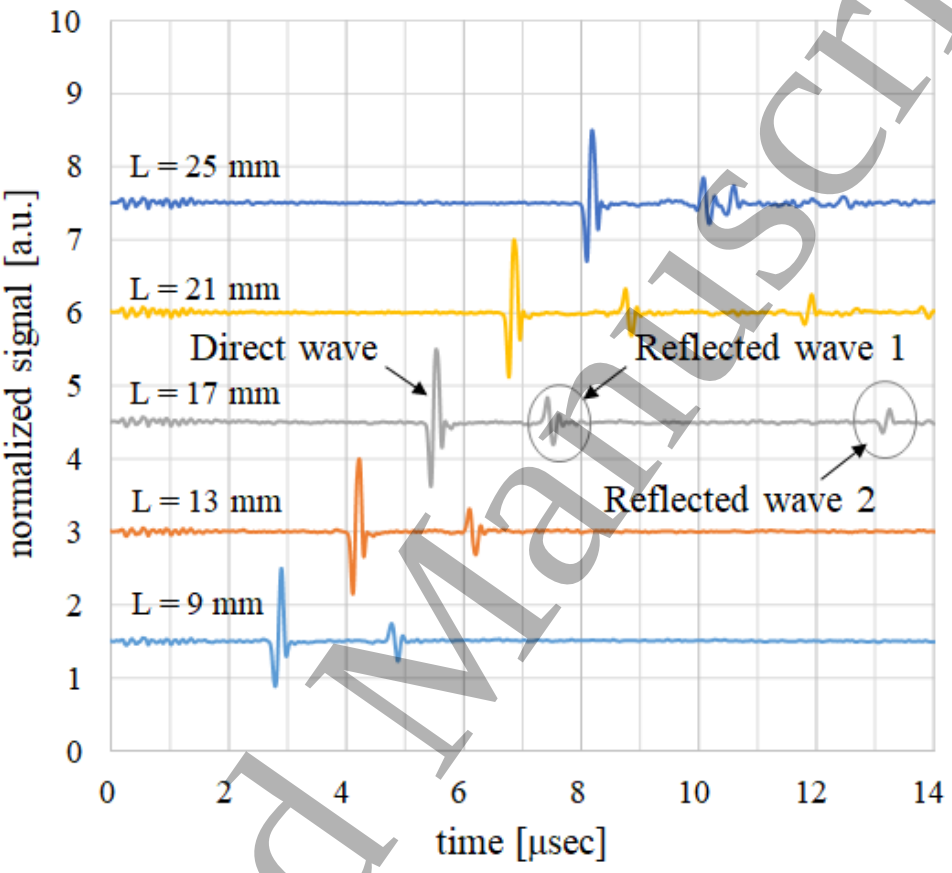

Fig. 4.

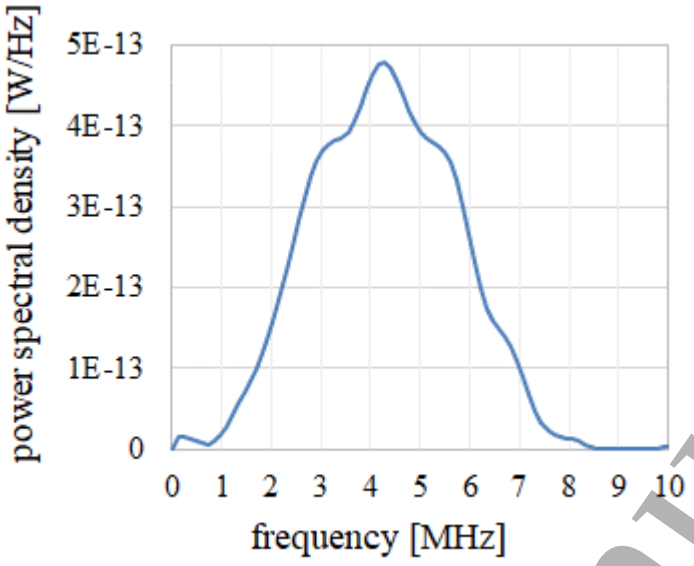

(a)

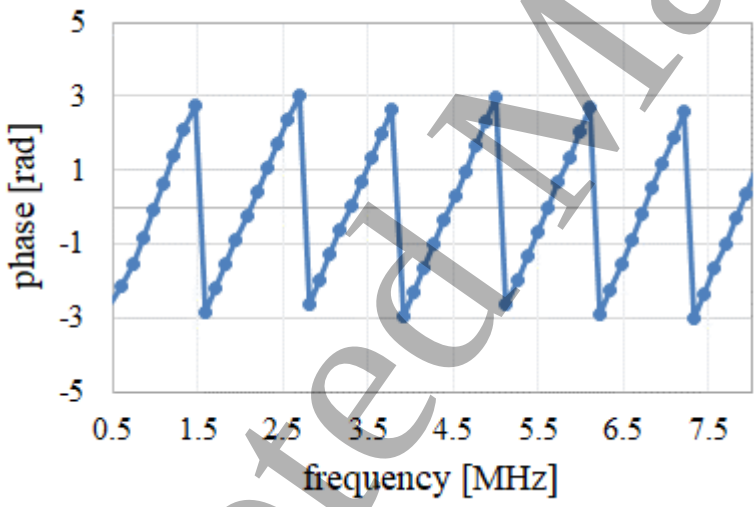

(b)

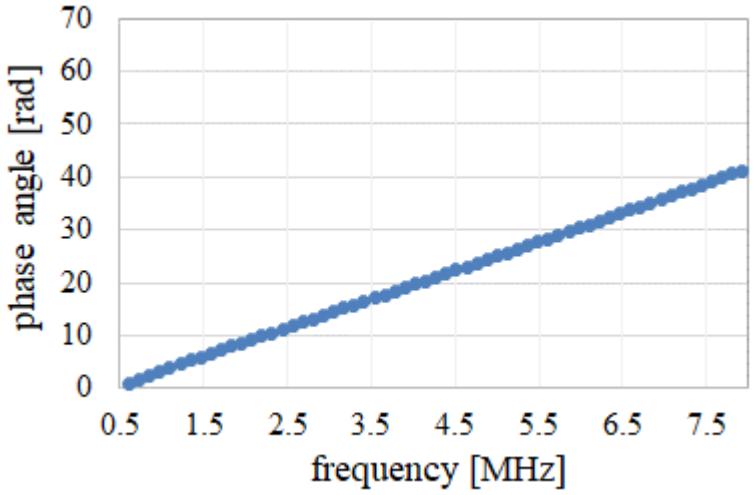

(c)

Fig. 5.

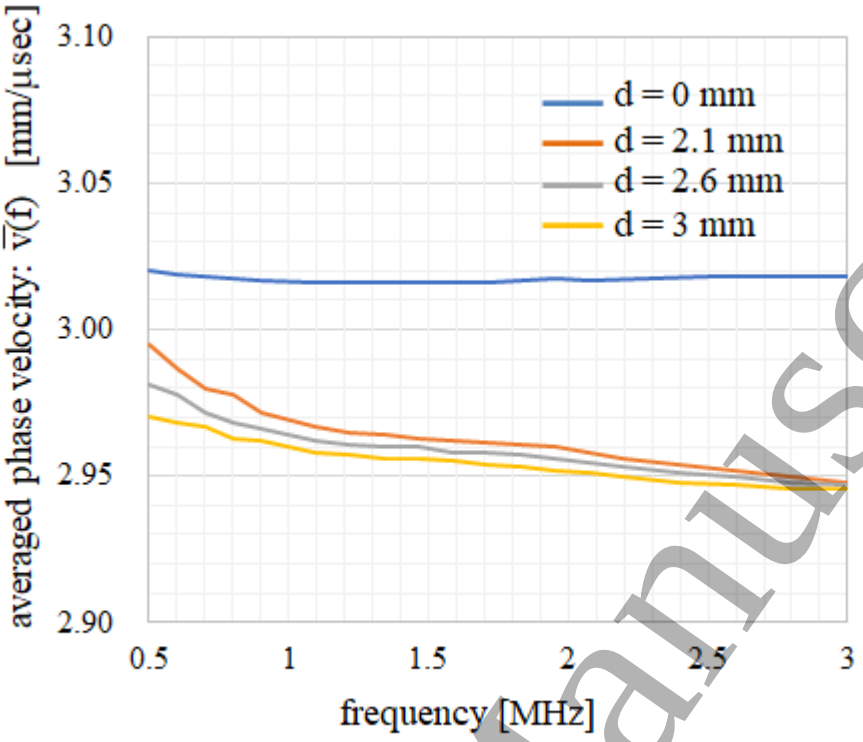

Fig. 6.

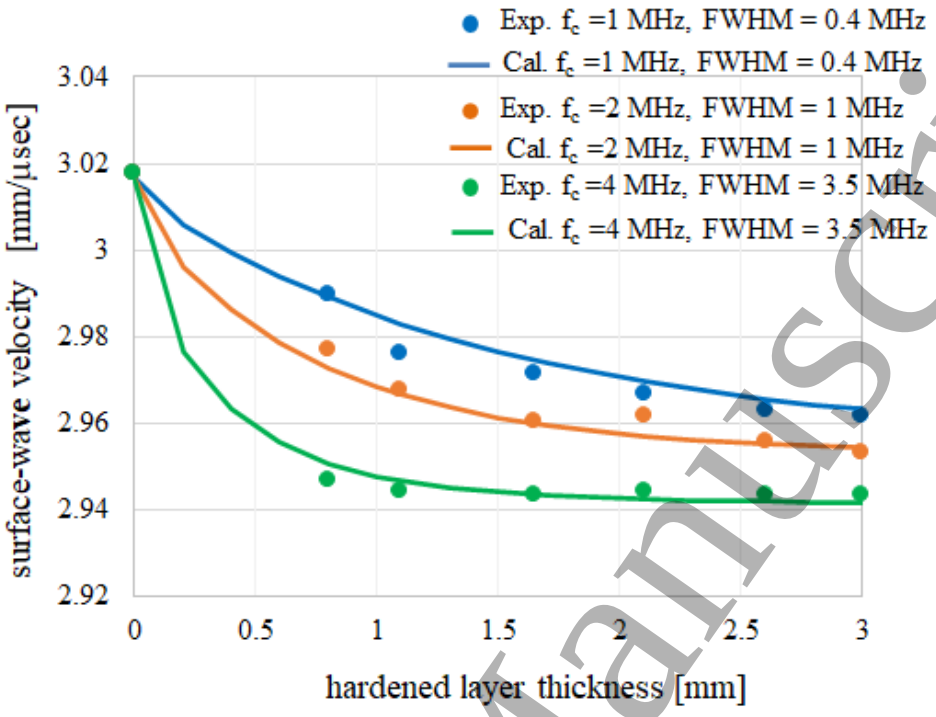

Fig. 7.

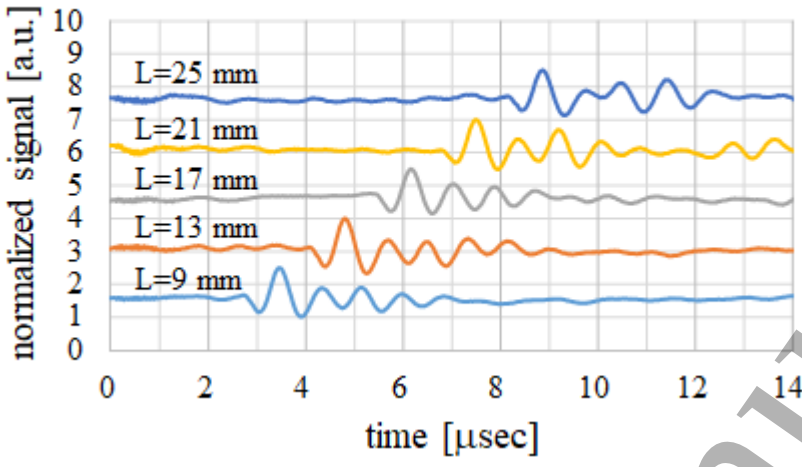

(a)

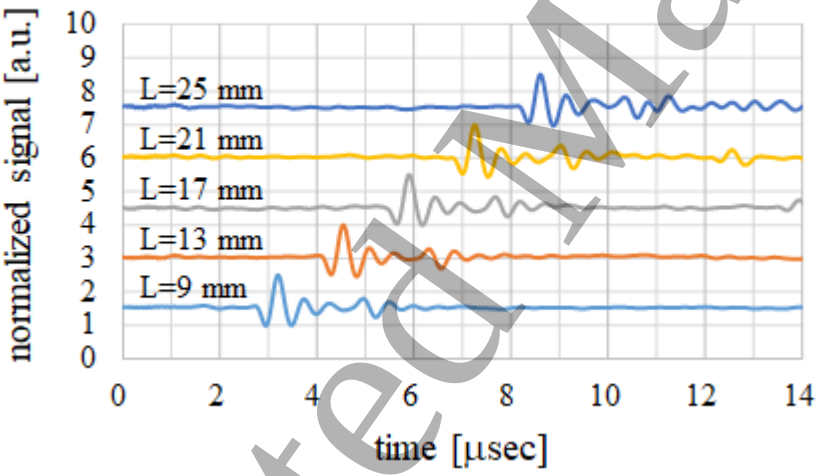

(b)

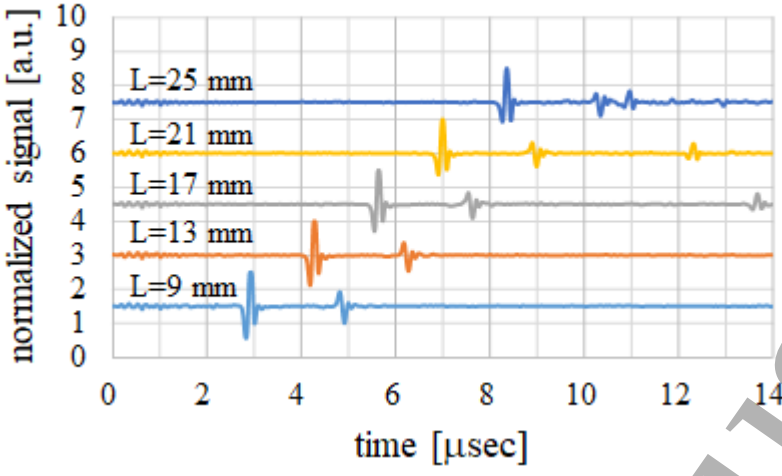

(c)

Fig. 8.

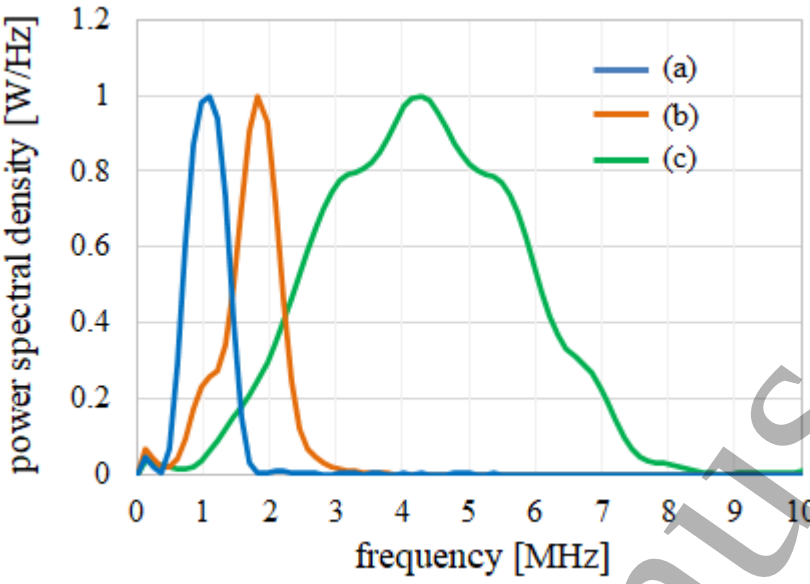

Fig. 9.

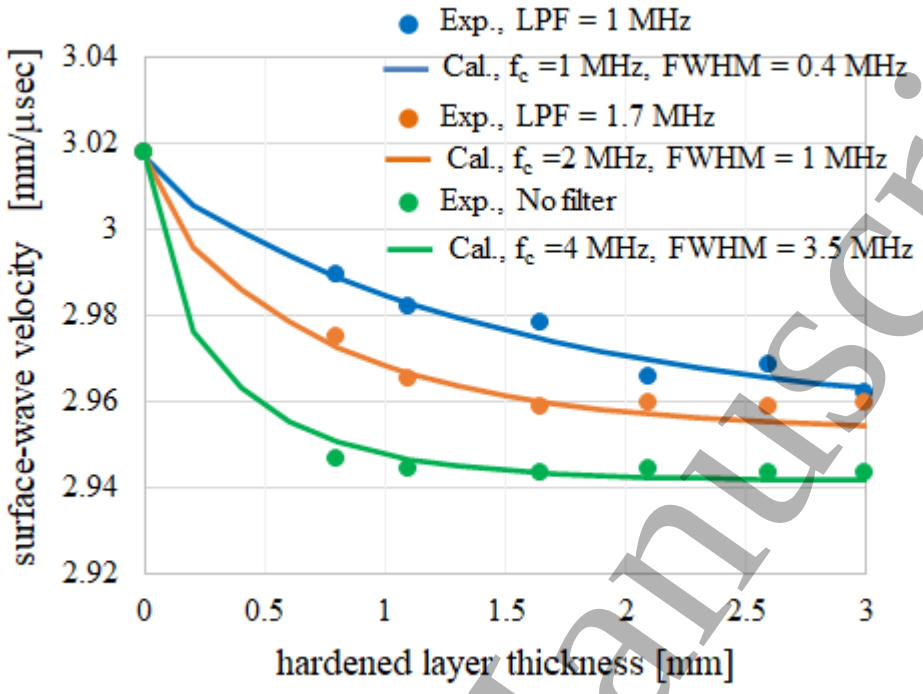

Fig. 10.